75th International Astronautical Congress (IAC), Milan, Italy, 14-18 October 2024.

IAC-24-A6.IP.64.x88651

SATELLITE AND RSO DETECTION, TRACKING AND ORBIT-DETERMINATION BY COMMERCIAL STAR TRACKERS IN REAL-SKY PERFORMANCE DEMONSTRATIONS AND ANALYTICAL CAPACITY ASSESSMENT FOR IN-ORBIT SSA APPLICATIONS

Andreas Hornig[a*], Uwe Schmidt[b], Thorben Haarlammert[a], Florent Bouillon[b], Simon Chelkowski[a]

[a] *Department of Space Situational Awareness, Jena-Optronik GmbH [01].*
[b] *Department of Programs, Jena-Optronik GmbH [01].*
* Corresponding Author, andreas.hornig@jena-optronik.de

Abstract

As the number of satellites in Low Earth Orbit (LEO) grows the risk of collision between them and the likelihood of un-consented rendezvous increases dramatically. This is threatening space as a resource and poses a challenge to Space Traffic Management (STM). Assessing the purpose of objects in a proximity approach will become more and more important within the scope of Space Domain Awareness (SDA). The U.S. Space Surveillance Network (SSN) currently tracks over 23000 Resident Space Objects (RSO) in LEO (at time of this paper) [02], including functional and decommissioned satellites and debris. The United States Government Accountability Office (GAO) predicts the launch of an additional 58000 additional satellites by 2030 [03]. The SSN uses ground-based sensors to monitor the activity in orbit, which limits the responsiveness of the satellite to react to threats.

On-board satellite sensors offer space-based alternatives to detect, track and identify satellites and other resident space objects (RSO). Jena-Optronik GmbH is a leading manufacturer of a product line of different commercial star trackers (CST) [09, 34] (ASTRO© product family), navigational cameras and LiDARs [04, 05, 38] (RVS© product family), as well as other Space Situational Awareness (SSA) sensors [17, 37]. In a recent effort, we expanded on feature updates on our star trackers to make space-based space object tracking possible to our customers‘ satellites. This enables the satellites to autonomously monitor their orbital surrounding for any object within their proximity and report any potential threat event to mission operation control and allows for autonomous reaction in the future.

In this paper, results are shown of the performance analysis of our three star trackers, the ASTRO CL [10], ASTRO APS3 [35] and the ASTRO XP [12, 36]. Their electronics and optics were designed to provide different classes of attitude performance, and with the algorithm update are now able to also detect and process satellites as seen as star-like objects. The paper presents the analysis of theoretical distance a 10cm (diameter) object can be detected visually by its magnitude. Furthermore, the results of ground-based real-sky tests are presented where different satellites (Starlink, Iridium,) and rocket-bodies are detected and identified as well as their apparent magnitudes were measured. The real-sky experiment also shows the accuracy of angular positioning with smaller than 0.01° angular position precision for the range of 500 km and the effects on the orbit determination of the tracked satellites. This performance is discussed within a comparison to other state-of-the-art systems and theoretical research.

The SSA features are developed within Jena-Optronik projects and the paper presents further applications relevant for satellite operators and for the STM as a whole.

Keywords:
Commercial star tracker, resident space object, detection and tracking, space situational awareness, space domain

Interactive Presentation of this paper:
Publicly available online via IAC/IAF website [41, direct link]

Related Paper & Presentation at IAC2024:
PRINCESS mission of the TU Berlin (code: IAC-24,B4,3,7,x86584, 2024-10-15 at 15:00 CEST, Space Hall 2)[31]

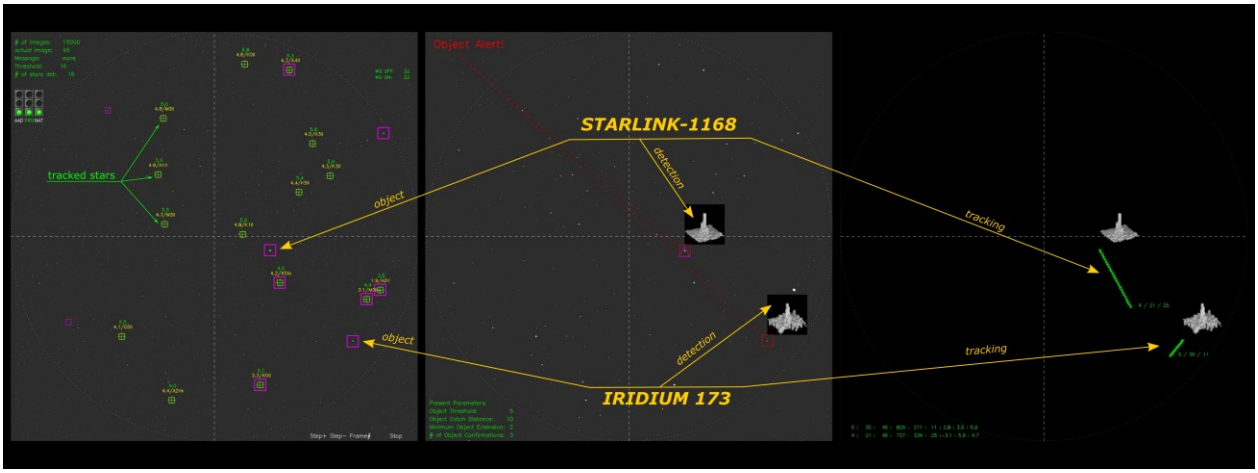

Fig. 0-1*: Jena-Optronik's Object Detection during robust Star Tracking NAT-Mode during a real-sky measurement with ASTRO CL star tracker.*
(left) Star Tracking Mode. (middle) Object alert of two objects between the celestial scenes with stars. (right) Object Tracking with two detected objects (object #3 and #5) with their pixel-data-block brightness distribution (small graphs) and the continuously tracked movement over the sensor's field-of-view (green track). Video here [41].

Acronyms/Abbreviations

The full list of acronyms and abbreviations can be found at the end of the paper.

1. Introduction

In the last two decades, an exponential growth in the number of satellites and other orbiting objects is happening (Fig.1-1, [02]). By the end of this decade, forecasts (such as the US-GAO report [03]) are showing trends with additionally tens of thousands new satellites being launched until 2030. Most of them are satellite for the LEO region. In addition to the active and passive satellites and launcher parts in orbit, the number of debris (diameter <1m) is also expected to follow in growth that is covered by ESA's DISCOSweb database [06] and adding to the number of resident space objects (RSO).

The sheer number of objects in orbits are posing a challenge for a coordinate space traffic management (STM) in the shared space called orbit of

- knowledge of existing objects and their behaviour
- analysis of short and long term effects such as proximities to other objects
- purpose and threat detection
- and finally coordinated, rule based counter measures, such as collision avoidance manoeuvres

Different ground based services exist for object detection and tracking via RADAR, LiDAR and optical instruments (individual and in a network). Space based instruments and sensors on-board of satellites recognizing any objects within reach is the next step enabling each satellite to detect and track objects. In this way the satellite itself is able to provide the resulting analysis directly to the satellite and the satellite's operator directly without time-delay of an external service provider. The operator or even the satellite in semi-autonomous modes is enabled to decide the purpose of the detected object. Either it can be a space debris that only requires additional monitoring. On the other hand it could be even another satellite that is conducting a consented optical surveillance and preparing a robotic rendezvous and proximity operations (RPO) for a scheduled in-orbit servicing. Or it is revealed to be an unconsented, un-cooperative RPO. The latter has been technically demonstrated in orbit since 2010 [07, 08].

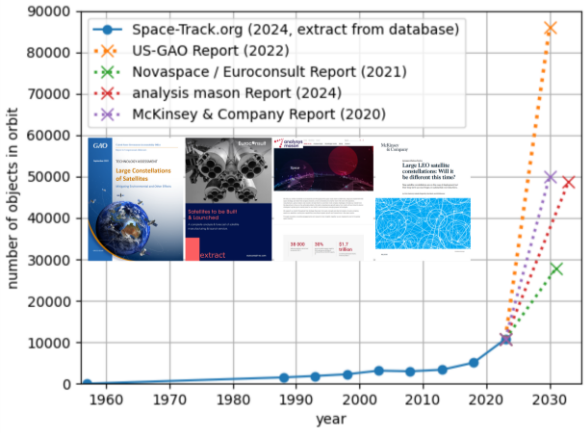

Fig. 1-1: Objects (satellites, rocket-bodies, debris, TBAs, ...) in Space-Track.org database (blue) [02] in orbit over the years, with trends of launched satellites by US-GAO[03] for 2030 (orange), by Novaspace/Euroconsult[60] for2031 (green), by analysis mason[61] for 2033 (red) and by McKinsey & Company[62] by 2030 (purple).

For future scenarios, a single satellite can be enabled for satellite protection to detect, observe and counter-act on basis of data from on-board sensors. The importance and relevance for satellite protection in civil and military purposes has increased significantly in recent years.

2. Commercial Star Tracker for RSO detection

For space-based RSO detection, commercial star trackers are well suited. They are deployed on each satellite and proven technology. And from the performance side, star trackers are optimized for capturing faint, spot-like light patterns such as stars and RSOs with similar patterns. Incidental RSOs that are illuminated by sunlight and are in line of sight of the STR are also often captured in these images.

2.1 Star Tracker vs. Payload Camera

For the determination of the attitude by stars, disturbances that could be interpreted as stars due to similar size, signal intensity and trackability but do not behave like expected from stars are ignored by the STR software. Detecting and tracking of RSOs that are appearing similarly to stars but do behave under a different prediction scheme require additional processing steps.

In contrast to a dedicated optical payload that is surveying for RSOs, the star tracker (STR) is continuously providing attitude solutions in form of quaternions towards the satellite's Attitude and Orbit Control System (AOCS), and additionally provide data of RSOs to the S/C. Both products, the attitude solution and the list of RSOs, can continuously be provided in parallel within the typical 0.1s integration time. A dedicated payload camera that would change to longer integration time of several seconds could lose the ability to attitude determination of each frame, for the AOCS and also for other image processing steps.

Commercial star trackers are typically deployed in sets of 2 or 3 star trackers per satellite. Their orientation to different directions, that minimize blinding by Earth, Sun and other sources of all sensors, allow a wider perimeter monitoring as with a single camera. This reduces blind spots for the satellite protection.

2.2 Solution by ASTRO CL as star tracker

Jena-Optronik GmbH (JOP) has a strong heritage in the development of opto-electronic sensors for numerous space-based applications. JOP is a market leader in providing optical cameras in form of star sensors [09] from commercial and scientific missions, as well as crewed missions (ARTEMIS [34]). Furthermore, with our Rendezvous- and Docking Sensors (RVS [38]) portfolio we are the worldwide leading company in the area of rendezvous- and docking operations in space [04].

In conclusion, JOP has the best pre-requisites to develop an optical SSA sensor suite [17, 37], which combines space-proven components including star trackers in a flexible manner to obtain one data set that covers the satellite surrounding perimeter volume and identifies incoming threats.

Within the ASTRO product line of commercial star trackers, the ASTRO CL for constellation, the ASTRO APS3 as an active pixel sensor with autonomous attitude solution, and the ASTRO XP [12] for extreme precision are available. All are based on the low noise and rad-hard FaintStar2 detector.

Fig. 2-1: Jena-Optronik's ASTRO product line. With ASTRO APS3, ASTRO XP and ASTROhead cam for scale for the ASTRO CL (in orange frame, 20° Near-FoV (left) and 68° Wide-FoV (middle), size of 1-Euro coin (right))

Table 2-1: ASTRO CL Star Tracker data*

"ASTRO CL (short for constellation) has been designed to fit the needs of LEO constellation spacecraft."	
Performance	
detector	FaintStar2 (low noise)
detector resolution	1020x1020 (12bit)
update rate	5Hz (full frame)
magnitude limit	5.8mi (with 0.1s integration time for star tracking)
Physical	
FoV	25deg (circular)
focal length	23mm
aperture / pupil	16mm (full)
operational I/F	SpaceWire (80MHz)
Environment	
radiation	up to 10 years in LEO and 15 years in GEO without additional shielding
Status	
units delivered	430 until August 2024
Missions	LEO constellations GEO platforms Smallsat & CubeSats

* full data sheet here [10] and paper [11]

The ASTRO CL (Fig.2-2, Table 2-1.) was selected for this capacity and capability assessment for detecting and tracking RSOs.

Fig. 2-2: ASTRO CL, the rad-hard, satellite constellation star tracker by Jena-Optronik is selected for this study.

Fig. 2-3: Two ASTRO CLs installed on ReflexAerospace's SIGI smallsat mission (image & info from reflexaerospace.com) to be launched on SpaceX Transporter-12 mission

For the real-sky experiment, the premises was that the ASTRO CL represents other commercial star trackers in this performance class. Furthermore, if it is able to detect and track RSOs, the higher performance classes such as the APS3 and AXP will be outperforming the ACL with respect to detection range and angular accuracy.

3. The Real-Sky Experiment with ASTRO CL

A measurement under real-sky condition was conducted. This experiment provided real data of objects that are visible during passage through the star trackers field of view. This was a blind observation without any a-priori knowledge of RSO target candidates. The goal was to detect, track and identify any RSO during a 1-hour observation with a CST. The ASTRO CL was selected due to its robust operation, its simplicity to work with any Laptop, and as a representative stand-in for the ASTRO line.

3.1 Location for observation

Jena-Optronik's headquarter is in the city of Jena, which is also known as "the optical valley" of Germany due to its favourable density of optical companies and tradition in this area. The measurement was conducted at a near-by observation point right outside the city and the valley (Fig-3-1) which has preferred light conditions for such an experiment.

Fig. 3-1: The City of Jena within Germany's Optical Valley (dotted line). Jena-Optronik's HQ [01] in the city and the observation location for the ASTRO CL's Real-Sky measurements at a proven location close by (Google Maps).

3.2 Set-up of Star Tracker

At the observation point, the ASTRO CL star tracker is oriented towards zenith (90° elevation) and fixed. No Earth motion compensation is used. With this orientation, the star tracker serves as a "satellite bucket" potentially catching light signatures from all satellites and objects flying through this FoV cone (Fig 3-2). The Earth's rotation make the stars in the background move slowly and they are used for the direct attitude-solving of each frame including all objects. The processing is conducted on full frame level on the laptop (UTNG software). Together with the time, geo-position and satellites orbital

parameter of this evening, the frames are stored for post-processing.

As a result, the attitude and object list are directly generated on frame basis. The object list is then matched with the TLEs and produces the confirmed satellite's list.

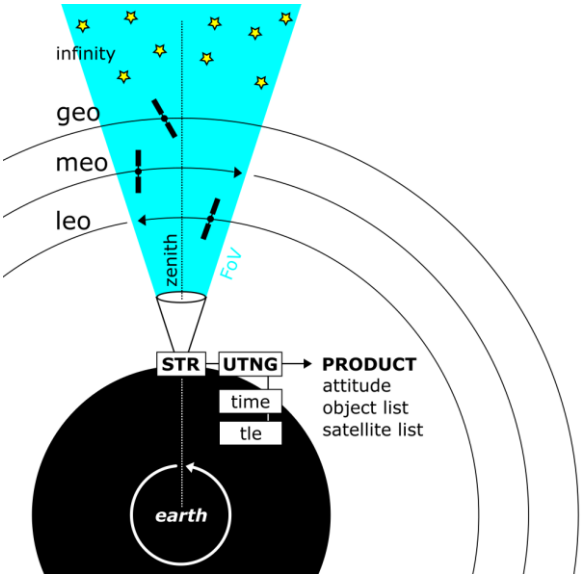

Fig. 3-2: Sketch of the measurement set-up. The ASTRO CL star tracker (STR) is on ground and fixed to zenith direction. The ACL is in NAT mode and observing satellite in its FoV. The data processing is performed on the UTNG computer. The resulting products are the continuous attitude solutions and an object list. The bright object lists is analysed for non-stellar objects that can be tracked according to their estimated paths on the detector. These candidate objects are matched to satellite TLEs[02] to identify the satellite's names and catalogue IDs.

3.3 Date, time and duration

The measurement started at 2022-03-08T19:00:45.04 (UTC) with a duration of 60 minutes. The astronomical twilight allows for phase angles that illuminate the objects so that they become visible, and the duration is long enough to cover the twilight duration so that enough satellites are flying through the sensor's FoV.

For this period, the TLEs of all objects in Space-Track.org [02] are used with the closest epoch to the start time.

4. Performance in RSO detection

The measurements are analysed under two aspects. Firstly, to validate the software-models for identifying the RSOs with existing objects from the Space-Track.org database and how the angular accuracy is between the sensor's object tracks and those of the reference TLEs. The direct real-sky experiment data is used for it. And secondly, the analytical assessment is extended to improve the software-model with closer to operational scenarios. The experiment results shall show how to configure an ASTRO CL and other FaintStar2 based star trackers to detect even fainter and further objects. This is a capability and limitation investigation.

4.1 Real-Sky Experiment

A total of 27 objects were tracked. An object qualifies as tracked when it was detected and then found by the estimator in 3 consecutive frames. Out of these, 22 objects could be matched with TLEs from Space-Track.org. These identified objects are part of this in-depth analysis.

4.1.1 Object Apparent Magnitude Patterns

The ASTRO CL provides the magnitudes of the objects based on the sensor's calibration for the visible spectral range. In Figure 4-1 all tracks are seen with most objects' apparent magnitudes around the magnitude level of 5mi. Due to the zenith position and the limitation of the 25° FoV, the orbital arches of the objects will neither change the distance, not the phase angle significantly. As a consequence, limited brightness jitter for the different objects is observed.

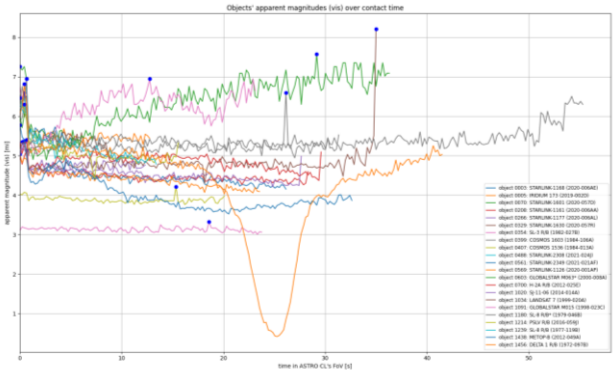

Fig. 4-1: Objects' apparent magnitudes (vis) over contact time. The faintest measurement per object is marked with a blue circle (larger legend in Figure 4-4)

The Delta 1 rocket-body is an obvious exception with its increase in brightness dip around its passage through the FoV center. Rocket-bodies (R/B) can be tumbling [30] and their cylindrical shape changes the effective cross section within a few seconds. This reflects and

radiates more light towards the observer for a temporary time, which is a likely reason here. With a wider FoV or a lower elevation expanding the observation time, a repetition of this change can reveal if it is a unique tumbling frequency.

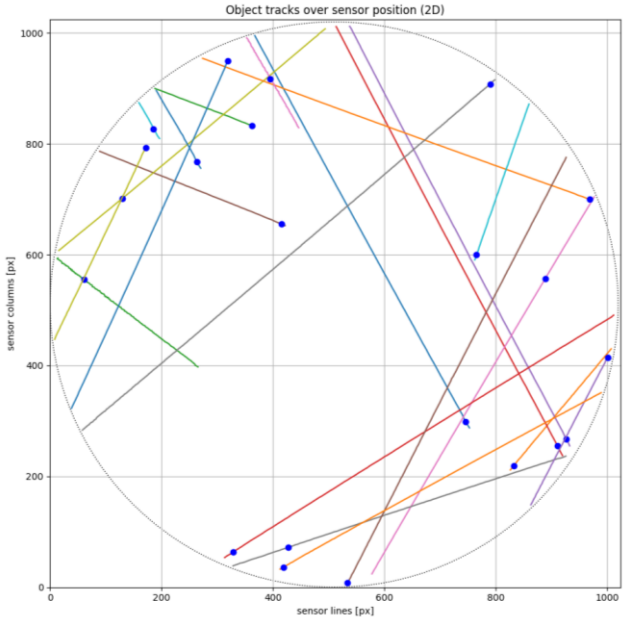

Fig. 4-2: Object tracks over sensor position (2D). The faintest measurement per object is marked with a blue circle. (legend in Figure 4-4)

The object tracks in Figure 4-2 show that the ASTRO CL provides sub-pixel accuracy of the objects positions which provides good tracking. A position noise reduced track is important for matching the measured track with the tracks simulated by the TLEs. The blue dots mark the maximum (faintest) magnitudes of each track and corresponds to the blue dots in Figure 4-1. Once tracked, the object were continuously tracked until loss. There was no re-acquisition required as there were no segmented tracks matched to the same TLE.

Figure 4-3 shows in a 3D-scatter plot the overview of magnitudes at sensor position. The dynamic range of the detector is used. The limiting magnitude of 5.8mi in star tracking mode and with 0.1s is reached. With the GLOBALSTAR M063 and M015 satellites, two objects' magnitudes increased above magnitude 7mi. These satellites are also those with the highest ranges and biggest average cross sections.

Further changes in brightness that could be related to flares (Iridium or Starlink) or tumbling of other rocket bodies is not visible.

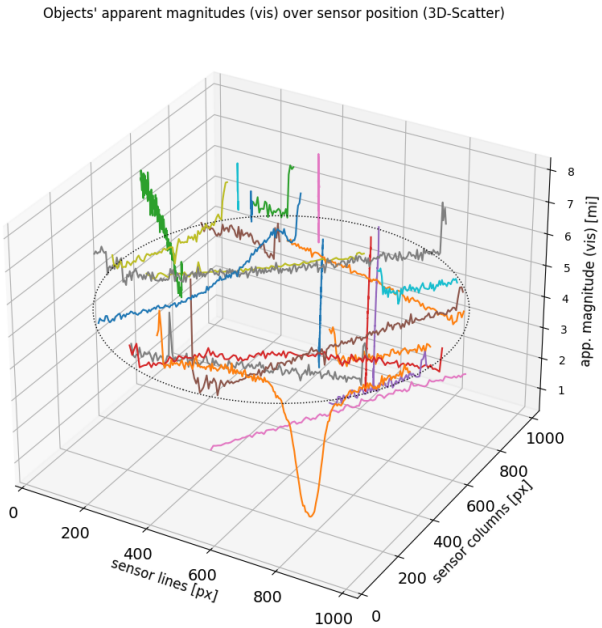

Fig. 4-3: Objects' apparent magnitudes (vis) over sensor position (as 3D-Scatter plot). Due to the zenith orientation of the ASTRO CL, most of the brightness stays in a constant range. The phase angle is not changing much within this FoV and time. The change of brightness that does occur can be seen for the OBJECT 1456 that is identified as a DELTA-1 Rocket Body which is tumbling and re-orientating that more cross section is projected towards the ASTRO CL for a few seconds. More light is redirected temporarily. (Legend in Figure 4-4)

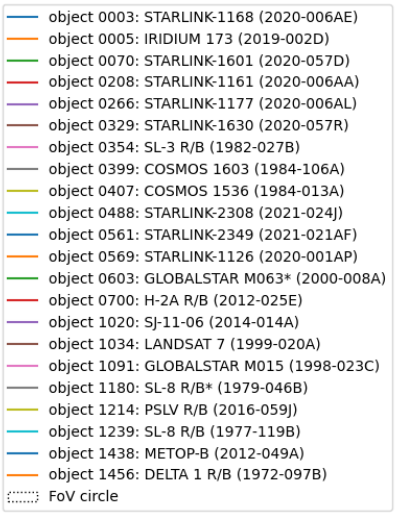

Fig. 4-4: The legend for the previous graphs for better reading convenience. The object list matches the object numbers from the detection to the identification of satellites, which is described in the next chapter.

4.1.2 Satellite Identification

Satellite identification is based on the RA/DEC values assigned to the objects based on the attitude solution of each frame by ASTRO CL software (See Fig.0-1). For each timestamp t of an object's track a RA/DEC pair is generated by each of the 28000 satellites' TLEs in Space-Track.org database for the experiment day. To find the closest match, the angular distance between the TLE and the measurement is computed (eq.1) via SkyField [20] and the smallest total error (eq.2) reveals the TLE candidate and thus the satellite that matches the closest the measured track [21].

$$\theta_t = \cos^{-1}\big(\sin(DEC_{tle_t}) * \sin(DEC_{meas_t}) + \cos(DEC_{tle_t}) * \cos(DEC_{meas_t}) * \cos(RA_{tle_t} - RA_{meas_t})\big) \quad \text{(eq.1)}$$

$$total\ error = Minimize \sum_t \theta_t \quad \text{(eq.2)}$$

The identified satellites for the 22 objects are listed in Table 4-1.

Table 4-1: Objects number from ASTRO CL with already identified Satellite or RSO with measured maximum Magnitude (faintest) and determined range

Obj.	Satellite / RSO	COSPAR	Range	Magn.*
#	*nation, name (r/b)*	*id*	*km*	*mi (vis)*
0003	STARLINK-1168	2020-006AE	556.31	5.34
0005	IRIDIUM 173	2019-002D	795.65	6.60
0070	STARLINK-1601	2020-057D	558.76	7.26
0208	STARLINK-1161	2020-006AA	561.78	5.13
0266	STARLINK-1177	2020-006AL	562.38	5.37
0329	STARLINK-1630	2020-057R	553.66	6.46
0354	*SL-3 R/B*	*1982-027B*	*540.53*	*3.33*
0399	COSMOS 1603	1984-106A	854.99	6.60
0407	COSMOS 1536	1984-013A	569.27	4.21
0488	STARLINK-2308	2021-024J	562.74	6.95
0561	STARLINK-2349	2021-021AF	559.45	6.51
0569	STARLINK-1126	2020-001AP	553.15	5.05
0603	GLOBALSTAR M063	2000-008A	1775.35	7.57
0700	*H-2A R/B*	*2012-025E*	*650.24*	*5.41*
1020	Shijian-11-6	2014-014A	726.29	5.36
1034	LANDSAT 7	1999-020A	721.93	8.21
1091	GLOBALSTAR M015	1998-023C	1942.23	6.95
1180	*SL-8 R/B*	*1979-046B*	*985.25*	*6.95*
1214	*PSLV R/B*	*2016-059J*	*724.14*	*6.46*
1239	*SL-8 R/B*	*1977-119B*	*780.43*	*6.30*
1438	METOP-B	2012-049A	845.36	5.78
1456	*DELTA 1 R/B*	*1972-097B*	*1124.52*	*6.82*

* Magnitude is taken at maximum (faintest) measurement and range is determined at time of maximum magnitude from Figure 4-1 (blue dot)

4.1.3 Satellite TLE time synchronisation

The satellite identification is done with TLEs that are having a 0-day bias of 1000m at epoch and a continuous increase of error [15,58] per time. That means that using the TLE of a satellite database for matching them to the measured tracks before a time-synchronization is possible as long as there are few satellites close to the measured track and creates an ambiguity. This ambiguity needs to be resolved with the decision criterion of angular distance between the measured positions towards the simulated position of the TLE. So situations arrive where there are several satellite TLEs that create close tracks to one measured track.

The 0-day bias leads to the simulated satellite being several seconds late or early on the expected RA/DEC location [18]. Mostly, the error is along track and not normal or lateral (see Fig.4-6, top).

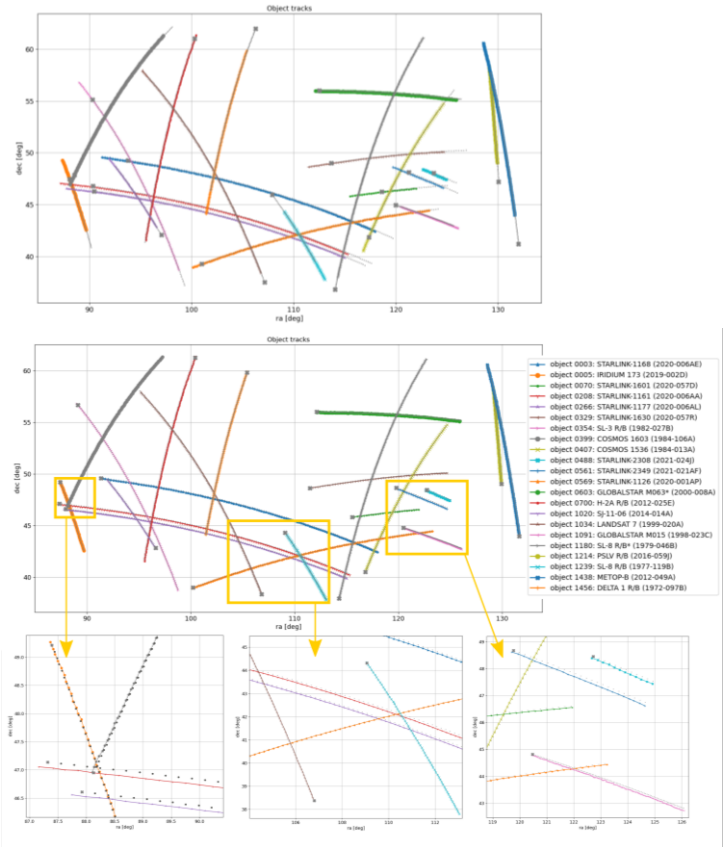

Fig. 4-6: Showing tracks in RA/DEC coordinate frames. Satellite tracks by TLE as dots, measured tracks as solid lines with different markers for object reference
(top) TLE tracks uncorrected by time offset. Starts are marked with X.
(bottom) Tracks corrected by time offset for each individual track. Result is closely matching the measured tracks. The X marks the first RA/DEC position of the satellite track.
(bottom zooms) Three examples from within the yellow boxed areas of how well the simulated tracks by TLE matches the measured tracks after time synchronisation. (zoom image in Appendix A-1)

A time offset for each of the identified TLEs can be performed shifting the simulated track closer to the measured track. This is done also with eq.1 and eq.2 to find the time offset. This allows to determine the angular truth between the measurement and the reference TLE (see Fig.4-5).

Table 4-2: Time offset* for the identified sat TLEs to measurement & 3D-RMS Orbit Determination results

Obj.	Satellite / RSO	TLE time offset	Range	Orbit 3D-RMS
#	*nation, name (r/b)*	*sec*	*km*	*km*
0003	STARLINK-1168	-2.15	556.31	3.348
0005	IRIDIUM 173	-3.357142	795.65	8.757
0070	STARLINK-1601	-2.942857	558.76	8.617
0208	STARLINK-1161	-2.835714	561.78	14.068
0266	STARLINK-1177	-2.407142	562.38	14.423
0329	STARLINK-1630	-1.978571	553.66	9.133
0354	*SL-3 R/B*	*-2.171428*	*540.53*	*0.677*
0399	COSMOS 1603	-2.0	854.99	2.495
0407	COSMOS 1536	-1.878571	569.27	0.971
0488	STARLINK-2308	-1.042857	562.74	1.741
0561	STARLINK-2349	-1.521428	559.45	2.887
0569	STARLINK-1126	-0.942857	553.15	14.068
0603	GLOBALSTAR M063	-0.935714	1775.35	2.938
0700	*H-2A R/B*	*-0.385714*	*650.24*	*3.413*
1020	Shijian-11-6	+1.392857	726.29	7.357
1034	LANDSAT 7	+1.535714	721.93	0.571
1091	GLOBALSTAR M015	+1.985714	1942.23	19.289
1180	*SL-8 R/B*	*+2.785714*	*985.25*	*4.008*
1214	*PSLV R/B*	*+3.028571*	*724.14*	*14.481*
1239	*SL-8 R/B*	*+3.442857*	*780.43*	*24.177*
1438	METOP-B	+5.492857	845.36	19.319
1456	*DELTA 1 R/B*	*+5.835714*	*1124.52*	*19.845*

* *Start 2022-03-08T19:00:45.04 (UTC), duration 60 minutes, TLE validity closest to the start time. (see Fig. 4-5)*

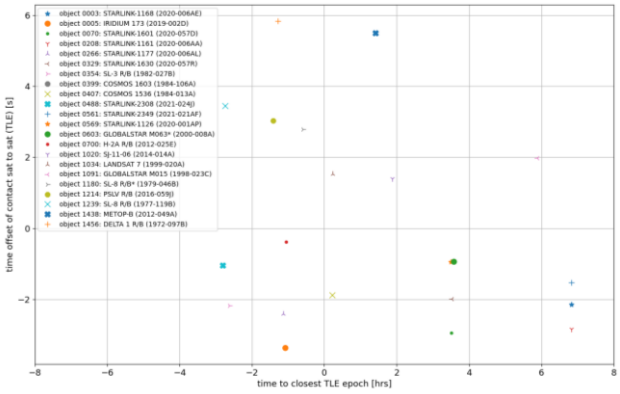

Fig. 4-5: Time synchronisation of all TLEs. The time offset of contact satellite to satallite (TLE). Offset between -3 to +6 seconds until the track by TLE matches better with the measured track. (see Table 4-2)

The tracks shown in Fig.4-6 match closely to the measurements tracks. Residual deviations in angular distance can be due to the 0-day bias. As seen in Fig.4-7, the total error and behaviour is different for each satellite. As an example for Starlink satellites, a 500m position error along track at a distance of 500km is an angular error of about 0.057° and in the range of the angular error seen in Fig.4-7. The measurements with the ASTRO CL reaches the effects by the validity of TLEs.

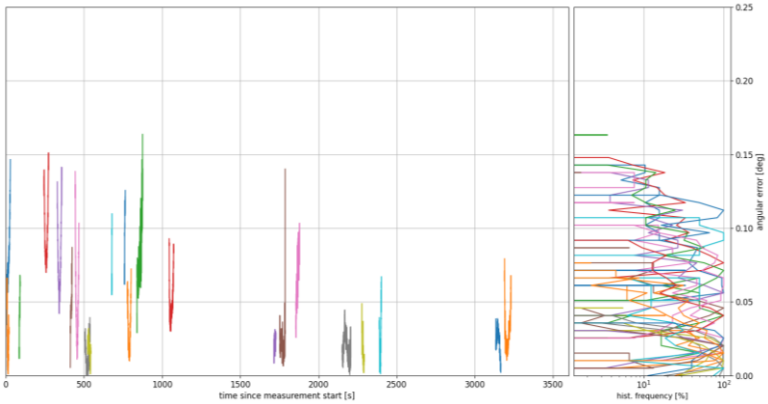

Fig. 4-7: Angular distance error (angular truth) over time (left) and their histograms (right). The error reaches 0.01° precision in histogram. (zoom image in Appendix A-2)

4.1.4 Preliminary Orbit Determination providing 3D-positions as final accuracy criteria

The main purpose of this assessment is to quantify the accuracy of the targeting of the RSO. Each object's RA/DEC track (Figure 4-6) is compared to the reference TLE by the RA/DEC angle. That gives only one part of the accuracy character based on angular temporal error noise. With TLEs beyond their validity, this is error prone. With applying preliminary orbit determination (OD) to the RA/DEC tracks, the integrity assessment is providing a better picture by deriving an orbital parameter set (Inc, RaaN, Ecc,…) and thus position (x,y,z) for each timestep from the angular (RA/DEC) measurements.

The OrbitDeterminator software [32] from the Distributed Ground Station Network (DGSN) project is used [33] and orbital parameters as TLEs are created. The created TLEs are compared to the reference TLEs via the 3D-RMS as the criteria of accuracy. This transfers the angular accuracy (angular truth) into 3D-position accuracy. Table 4-2 shows all results and Figure 4-8 shows one result of the OrbitDeterminator software for "LANDSAT 7". It applies a 6-DoF-optimizer on about 14-16 timely-equally distributed track points and minimizing a likelihood sum of the 6 orbital parameters that that are shown (except True Anomaly).

The 3D-RMS results are quite good from a few km to within the TLE 0-day bias of a few 100 meters.

Improvement is possible as it is typical for such input data of

- angles only (RA/DEC) measurements as input
- one pass/arc of an object (not several passes)
- observed from only one location
- small FoV that provides a small angular width (not horizon to horizon view)

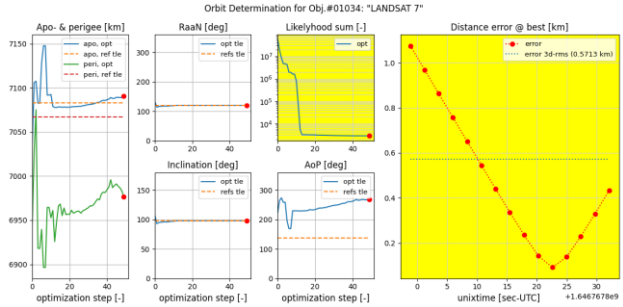

Fig. 4-8: Result of Object #01034 "LANDSAT 7" from OrbitDeterminator tool [32]. Angular distance error (angular truth) over time (left) and their histograms (right). The error reaches 0.01° precision. (zoom image in Appendix A-2)

The typical and expected behaviour of matching RaaN and Inclination, and bigger differences in Apogee and Perigee altitudes, as well as the Argument of Perigee (AoP) is visible in Figure 4-8, because as the optimizer matches only a minute of measurements of a 90+ minute orbits. So this part of the geometry has the expected smallest distance error.

As this is an expected behaviour, with 3D-RMS that allows SSA applications, and can be improved by more measurements, preliminary orbit determination is possible with the ASTRO CL star tracker for satellite protection.

4.2 Analytical Assessment

4.2.1 Evaluation of Real-sky Measurement

A total of 27 objects were tracked. An object qualifies as tracked when it was detected and then found by the estimator in 3 consecutive frames. Out of these, 22 objects could be matched with TLEs from Space-Track.org. These identified objects are part of this in-depth analysis. The analysis will show how the satellites that are very diverse in size, orbit, optical & radiative properties, operation modes and many more parameters can be compared. This is performed by norming them to a representative diameter size of 10cm, which is a typical size that use widely used for performance comparison within the SSA community. For that, it is of utmost importance to have the satellite candidates identified to allow extracting the mentioned parameters from other databases and norming them.

With the matched satellite TLEs, the range from the observation point to the satellite at the time of maximum (faintest) magnitude is extracted for each object. Figure 4-9 shows the 22 objects with most of their ranges of 500-600km as most satellites are in LEO. The furthest object range is about 2000km and it also is close to the cut-off magnitude for the 0.1s integration time.

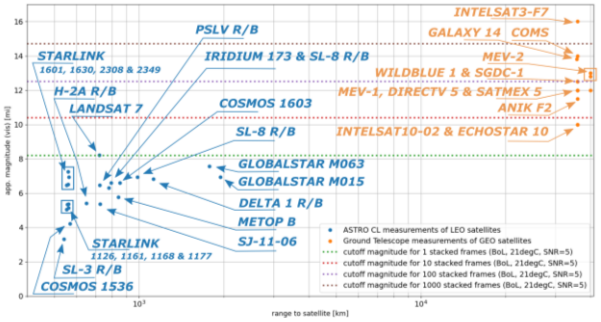

Fig. 4-9: Object magnitude (blue) by ASTRO CL over range. For comparison GEO satellite magnitudes (orange) from ground based telescope surveys. Counts of stacked ASTRO CL images for orientation of cut-off magnitudes (horizontal lines).

4.2.2 Extension towards norming the results to 10-cm standard size

The matched satellite sizes vary, and so does their phase angle, orientation and more that does effect light radiation towards the observation point. So the satellites sizes are normed (eq.3) to a 10cm diameter which is a good stand-in for a typical debris or to a 1U CubeSat (Fig. 4-10). The basis for the original size is taken from ESA's DISCOSweb [06] as the average cross section (acs, or x-section).

$$R_{norm} = \frac{R_{sat}}{r_{sat_{cs}}} * r_{norm} = \frac{R_{sat}}{r_{sat_{cs}}} * \frac{\mathbf{0.1m}}{2} \qquad \text{(eq.3)}$$

Table 4-3 allows now to compare in a better way the performance of the ASTRO CL for RSO detection and tracking while operating in star tracker typical configuration (integration time of 0.1 seconds, attitude solution output). Furthermore Table 4-3 also includes GEO satellites with their normed ranges based on their ground based telescope surveys.

Table 4-3 and Figure 4-11 show the normed ranges for the different magnitudes.

Table 4-3: Objects number from ASTRO CL with already identified Satellite or RSO with measured maximum magnitude (faintest) and determined range

Satellite / RSO	avg. X-section	Range (sat)	Range (norm)	Magn. *
name, R/B, deb	*m^2*	*km*	*km*	*mi (vis)*
STARLINK-1168	13.5615	556.31	13.39	5.34
IRIDIUM 173	14.4232	795.65	18.57	6.60
STARLINK-1601	13.5615	558.76	13.45	7.26
STARLINK-1161	13.5615	561.78	13.52	5.13
STARLINK-1177	13.5615	562.38	13.53	5.37
STARLINK-1630	13.5615	553.66	13.32	6.46
SL-3 R/B	*10.4143*	*540.53*	*14.84*	*3.33*
COSMOS 1603	38.4845	854.99	12.21	6.60
COSMOS 1536	13.2170	569.27	13.88	4.21
STARLINK-2308	13.5615	562.74	13.54	6.95
STARLINK-2349	13.5615	559.45	13.46	6.51
STARLINK-1126	13.5615	553.15	13.31	5.05
GLOBALSTAR M063	5.5868	1775.35	66.56	7.57
H-2A R/B	*35.1858*	*650.24*	*9.71*	*5.41*
SJ-11-06	2.0453	726.29	45.01	5.36
LANDSAT 7	18.7424	721.93	14.78	8.21
GLOBALSTAR M015	5.5868	1942.23	72.82	6.95
SL-8 R/B	*14.6461*	*985.25*	*22.82*	*6.95*
PSLV R/B	*6.1850*	*724.14*	*25.80*	*6.46*
SL-8 R/B	*14.6461*	*780.43*	*18.07*	*6.30*
METOP-B	37.4920	845.36	12.24	5.78
DELTA 1 R/B	*6.0475*	*1124.52*	*40.52*	*6.82*
REFERENCE SATELLITES FROM GROUND BASED TELESCOPES				
INTELSAT3-F7 [22]	1.952	36000	2283.53	16.0
COMS [23]	13.625	36000	864.33	14.0
SGDC-1 [24]	34.994	36000	539.33	12.5
GALAXY 14 [25]	20.000	35780	709.04	13.8
MEV-1 [04, 26-28] **	29.373	36000	588.67	12.0
MEV-1 [04, 26-28] **	29.373	40000	654.08	12.0
MEV-2 [04, 26-28] **	29.373	40000	654.08	12.8
MEV-2 [04, 26-28] **	29.373	40000	654.08	13.0
INTELSAT10-02 [28]	31.072	40000	572.35	10.0
WILDBLUE 1 [29]	34.556	36000	542.73	12.5
ANIK F2 [29]	67.277	36000	388.97	11.5
DIRECTV 5 [29]	40.765	36000	499.69	12.0
ECHOSTAR 10 [29]	49.678	36000	452.65	10.0
SATMEX 5 [29]	55.805	36000	427.08	12.0

* Magnitude is taken at maximum (faintest) measurement and range is determined at time of maximum magnitude from Figure 4-1 (blue dot)

**MEV-1 is based on Orbital Sciences GEOstar small geo bus [27]. As there are no avg. x-sect. values for MEV-1 and -2 in the DISCOSweb database, the GEOstar based SES-18 values are used as stand-ins [45].

For the 0.1s integration time configuration, the ASTRO CL can detect most 10cm objects at normed ranges around 13km with a magnitude of 5-6mi. This is due to the fact that most objects revealed themselves as Starlink satellites which share the same orbit parameters (and thus the same range) and all of these are the same built version v1.5 [16,59] which share the same average cross section on DISCOSweb. The furthest normed range is about 73km for the GLOBALSTAR M015 (as a normed 10cm object).

All these measurements were conducted with a maximum integration time of 0.1 seconds (Figure 4-11, green horizontal line). By keeping the advantage of attitude solving per frame for an AOCS but also using stacking of several images, the SNR can be increased to detect even fainter objects. The listed GEO satellites become possible to be detected with the ASTRO CL by stacking between 10 and 100 of these 0.1 seconds frames. With these effective integration times of 1 to 10 seconds for an ASTRO CL, it is similar to the different methods of exposure time of several seconds other ground based telescopes and other space based payloads apply.

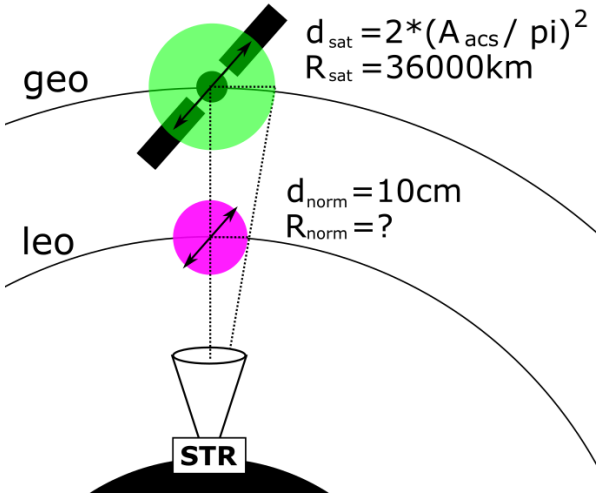

Fig. 4-10: A sketch of norming the satellite size of a GEO satellite to a typical 10cm diameter debris. Comparing the different satellites by their ranges to the same cross section. The average cross section (acs) area (A) is taken from ESA's DISCOSweb[06] and the satellites ranges (R) are taken from the Space-Track.org[02] database and further sources.

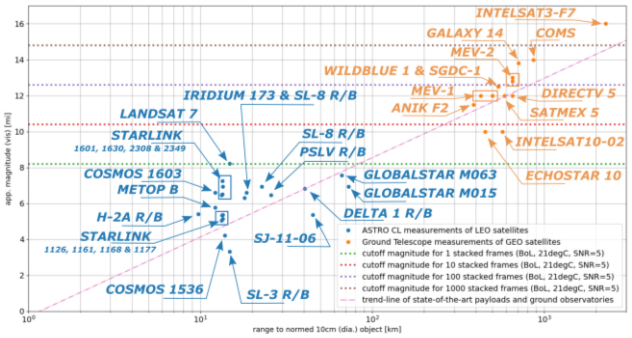

Fig. 4-11: Object magnitude (blue) by ASTRO CL over normed range for a 10cm diameter object. For comparison GEO satellite magnitudes (orange) from ground based telescope surveys also as 10 cm dia. sizes. Counts of stacked ASTRO CL images for orientation of cut-off magnitudes (horizontal lines). Magnitude trend line (purple)

$$Mag_{trend} = 1.9192 * LN(R_{rso\_in\_km}) - 0.2927 \text{ (eq.4)}$$

A meta-analysis trend of about 100 sensor sensitivities by public papers and data sheets is shown in Equation eq.4. It gives a magnitude trend for ranges for detecting a 10cm diameter sized object. In Figure 4-11 it can be seen following through the ASTRO CL measurements, where the measured magnitudes are mainly above the trend line, and leading to the GEO satellites plausibly.

4.2.3 Transfer of performance to other star trackers

The trend line together with the stacked frames (in number and total seconds) can serve as a predictor for modelling the Signal-to-Noise (SNR) behaviour and the detection capability of the ASTRO CL for other integration times, or it is used for the ASTRO APS3 and ASTRO XP to validate their performance based on their wider aperture diameters and at what ranges they can detect objects with a specific magnitude by integration time and SNR.

The nightly real-sky experiment was conducted with the ASTRO CL. With the ASTRO APS3 and ASTRO XP, Jena-Optronik has two further commercial star trackers that are based on the FaintStar2 sensor. The magnitude trend of Figure 4-11 allows to estimate the expected distance performance of these two CSTs with their reachable magnitudes also with 100ms integration time for star tracking mode. Table 4-4 shows this for the normed 10cm object and for Starlink satellites. Similarly to the ASTRO CL, stacking of frames are extending the range depending on the RSO of interest.

Table 4-4: ASTRO camera expected distance performances to typical 10cm objects and Starlink satellites (for star tracking SNR=10. With SNR of 5 and 3, respective magnitudes will still allow to detect objects at even further ranges)

		ASTRO line		
		CL[10]	**APS3**[35]	**XP**[36]
FoV (circular)	°	25.0	20.0	3.3
Magnitude for 0.1s integration time	*mi*	5.8	7.0	9.5
SNR basis		10	10	10
Range for observation				
…of a 10cm object*	*km*	23.9	44.7	164.4
…of a Starlink**	*km*	994.0	1857.5	6833.7

* *determined with eq.4, which is conservative*
** *determined with eq.3, via 10cm (dia.) object range*

Table 4-5: Ranges* for ACL, APS3 and AXP based on trend magnitude (eq.4) and SNR=10

Satellite / RSO* as 10cm (dia.) discs	Range (ACL)	Range (APS3)	Range (AXP)	Magn.*
name, R/B, deb	*km*	*km*	*km*	*mi (vis)*
STARLINK-1168	18.8	35.2	129.4	5.34
IRIDIUM 173	36.3	67.8	249.5	6.60
STARLINK-1601	51.2	95.6	351.9	7.26
STARLINK-1161	16.9	31.5	116.0	5.13
STARLINK-1177	19.1	35.7	131.4	5.37
STARLINK-1630	33.7	63.0	231.9	6.46
SL-3 R/B	*6.6*	*12.3*	*45.4*	*3.33*
COSMOS 1603	36.3	67.8	249.5	6.60
COSMOS 1536	10.4	19.5	71.8	4.21
STARLINK-2308	43.5	81.4	299.4	6.95
STARLINK-2349	34.6	64.7	238.0	6.51
STARLINK-1126	16.2	30.2	111.2	5.05
GLOBALSTAR M063	60.2	112.4	413.5	7.57
H-2A R/B	*19.5*	*36.5*	*134.2*	*5.41*
SJ-11-06	19.0	35.5	130.7	5.36
LANDSAT 7	84.0	156.9	577.2	8.21
GLOBALSTAR M015	43.5	81.4	299.4	6.95
SL-8 R/B	*43.5*	*81.4*	*299.4*	*6.95*
PSLV R/B	*33.7*	*63.0*	*231.9*	*6.46*
SL-8 R/B	*31.0*	*58.0*	*213.4*	*6.30*
METOP-B	23.7	44.2	162.7	5.78
DELTA 1 R/B	*40.7*	*76.0*	*279.8*	*6.82*

* *Ranges are meant to be compared for the 10cm representation of these RSOs*

Table 4-5 represents the ranges as if the satellites were seen from the ACL, APS3 or AXP by their magnitudes. When the magnitudes and the SNR of 10 with 0.1s integration time of each star tracker is applied to eq.4, the performance estimation for the 10cm (dia.) representative of the referred satellite is presented.

5. Applications in SSA Missions

The ASTRO CL is designed as a space-based sensor on-board of satellites. Its design makes it flexible to work as a star tracker and as an SSA camera. The low cost favours multi-camera systems for extending the perimeter view around a satellite or even from one satellite to another satellite within the same swarm.

This chapter gives an overview where such an STR enables applications (Overview in Table 5-1, and Figure 5-1 for market solution).

Table 5-1: ASTRO CL as an SSA sensor - overview

SSA Applications	ASTRO CL
Satellite Protection	yes
Sustainable & Clean Space	yes
Navigation	yes
Space Surveillance & Traffic Management	yes*

* *possible, depending on the satellite and operation*

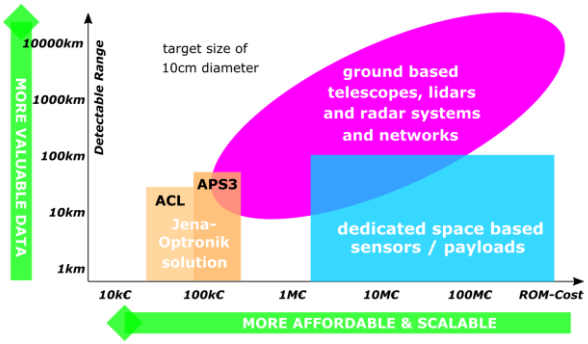

Fig. 5-1: Solution cost and detectable range of a 10 cm object (diameter) size generalized trade-off for current and the proposed Jena-Optronik solution

5.1 Satellite Protection

With ranges of 73km for an observed 1U cubesat size, RPOs can be detected and counter-measured like evasive manoeuvres can be started by the satellite's operators. Within this distance, the RPO conducting satellite still takes several fraction of a half co-phasing-orbit to be within contact vicinity.

Even before RPO, observation phases of one satellite to another were demonstrated with distances closer than 73km [07]. During these intelligence gathering phases, the ASTRO CL as an SSA sensor would be able to detect and assess the situation several hours before the identified RPO satellite is initiating to close in. The satellite operator can decide on this basis.

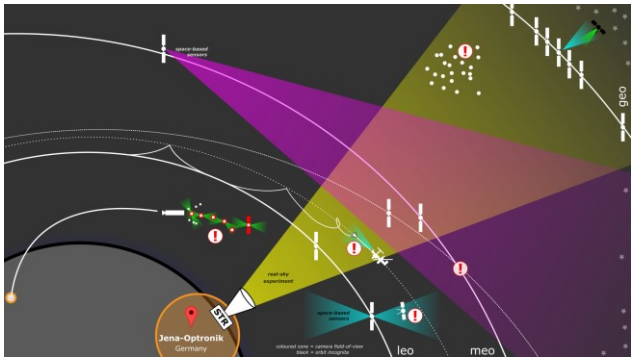

Fig. 5-2: Sketch with all supported SSA applications for a commercial star tracker.

Each (!) marks one of the applications of this paper section and is shown in zoom in the interactive presentation [41].

Shown are: satellite protection in blue cones, space-traffic management in purple cone, navigational applications within rideshare trains/swarms or for ISS docking in green cones, and general object tracking (satellite or debris) in yellow cone.

5.2 Sustainable, Clean Space & Mitigation

The ACL is able to detect and track relevant space debris also smaller than 10cm diameter at a closer range. Firstly, space debris that is on collision course on the same orbit is potentially detectable. But secondly, the ACL can support the documentation that the own satellite or launching vehicle did release a particle that then becomes a debris (the launcher's release adapters, paint chips, other lose parts). With more recommendation and regulations of sustainability in space, this becomes relevant (Fig.5-2, green and yellow cone).

As a calibrated sensor, the ACL provides information of brightness of objects. This enables sensor networks to validate the effectiveness of mitigation techniques applied by the satellite manufacturers and operators to reduce disturbing effects on other astronomical telescopes.

> "***The International Astronomical Union (IAU) expressed concern about the negative impact that the planned mega-constellations of communication satellites may have on astronomical observations and on the pristine appearance of the night sky when observed from a dark region***" [IAU, 39].

The ACL is able to detect the systematic change of brightness of the mitigation scheme for the Starlink satellites [46-49]. In Figures 4-9 and 4-11 it is clearly recognizable, that there are two clusters of brightness levels at one about 5.5mi and the other at about 6.5mi. Starting with Starlink number 1436 [40], SpaceX implemented the "Visorsat" configuration that dimmed down the reflectiveness of the satellites via the outer hardware and with a modified flight operation of orientation [47, 48]. Implementing ACLs in such regulatory validation networks (ground based SSN, see section 5.4), that are documenting the behaviour of satellites, allows for an automated and coordinated process and control of the orbits as a shared medium and induced "light pollution".

5.3 Navigation

In navigation, the ASTRO CL enables two kind of missions. The relative manoeuvring of two docking satellites and the orientation within a group of satellites. For both missions, the relative angular accuracy towards the other satellite is provided by the SSA sensor. When the target satellite is detected by its star-like properties on the 1020x1020 pixels of the detector, a sub-pixel accuracy of ~8arcsecs is possible within the 20° FoV to be used to control and maintain the satellite orientation towards the target. Either for keeping the orientation

within formation in a swarm by reaction wheels steering, or for a controlled and propelled flight within a corridor towards the docking partner. Both can be achieved by angular measurements only and using the pixel coordinates as the input for the steering control.

For relative manoeuvring, the ASTRO CL is selected for the PRINCESS (Precise In-Orbit Collision Prediction and Space Environment Surveillance System) mission proposal of the Technical University of Berlin [13, 14, 31]. There, two ACLs are deployed on the so-called "PRINCESS" mothership small satellite which is derived from the spacecraft currently developed for the "*QUantentechnologien für den Einsatz auf Einem Nanosatelliten*" (QUEEN)[43] mission at Technical University of Berlin. The ASTRO CLs serve to detect and track two Free-Flyers (3U cubesats) deployed together with the Mothership into orbit and that both perform individual propulsion missions in close vicinity of the mothership (Fig.5-4).

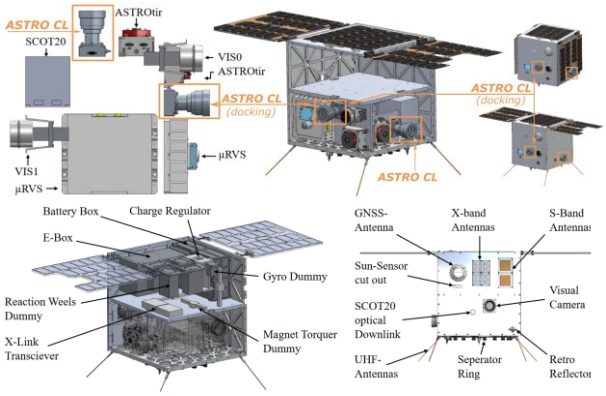

Fig. 5-3: PRINCESS satellite:
(top) CAD model of the Mothership with payload configuration in deployed and stowed state. The optical payload VIS1&0, next to the JOP optical sensors (ASTROtir, uRVS and ASTRO CLs [in orange boxes]) and the optical communication terminal (SCOT20) [44].
(bottom) Mothership with bus components and communication side view. [13, 14, 31]

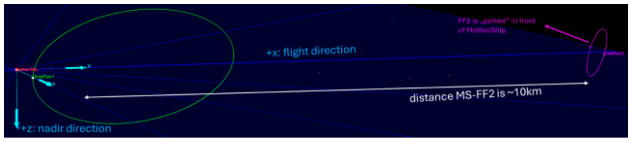

Fig. 5-4: 3D visualisation of NASA GMAT simulation of the relative orbits between both Free-Flyers and the Mothership [13, 14]

This mission includes also docking to the Mothership using bio-inspired docking adapters that resemble the skin features on the feet of Geckos. During all phases, the ACLs are used to support the relative manoeuvres by providing the position to the ground operations and also to the Free-Flyers inter-satellite link. In this way, the ACL is a navigation cam (nav-cam) (Fig.5-3).

For the group orientation, there are two scenarios of importance for the ASTRO CL as a nav-cam (Fig.5-2, green and blue cone).

When the satellite is released as part of a rideshare mission and the satellite moves within a "satellite train" with a high and dense number of other satellites, the ASTRO CL can provide the orientation of the train position. This is a difficult task to find out which satellite is which, and certain next mission steps require knowledge which satellite is the own one and how much distance is to the next satellite. The orbit determination analysis provides strong evidence that satellite orbits can be obtained in the range of a few hundred meters (3D-RMS for arcs). This allows for gnostic information of each neighbouring satellite in the train reducing the identification and TLE assigning from days to mere hours. Earlier commissioning the satellite into commercial service becomes possible [58].

Furthermore, for swarm or cluster missions with several satellites working together (such as Earth observation, geodesy, and multi-sensor products), the relative orientation towards the other satellites within the swarm or cluster is needed for any satellite. Each satellite can optically find the others and orientate correctly towards them.

And lastly, this supports de-orbit missions where in-orbit servicing missions are docking on other co-operative or are catching un-co-operative satellites to extend the mission [04], or initiate the Phase-F disposal and de-orbit the satellite [42]. To achieve this, orbital knowledge as 3D-position of the target at a future time is needed for rendezvous, and the relative angular accuracy for the docking phase at close vicinity at the target is required. Both are needed for targeting the docking partner and to transfer targeting from a few hundred meters at further distances, to sub-meters when reaching coupling distances.

5.4 Space Surveillance Networks & Space Traffic Management

With a wide installation basis of ASTRO CL star trackers in space (430 delivered by August 2024, Table 2-1), their data can serve as inputs for different Space Surveillance Networks. The SSN includes the space based data to improve their orbital knowledge and provide this for space traffic management (STM). For that, the ASTRO CL output product of the satellite list needs to provide RA/DEC with timestamps for orbit determination. The ASTRO CL can provide this with 0.01° angular precision. (Fig.5-2, purple cone).

From an individual satellite's operation, the ASTRO CL as an SSA sensor allows to conduct the manoeuvres planned with the STM. The STM provides the overview of all other objects including the one that for example a collision risk alert. The maneuverer is planned according to this risk and the future risk after the maneuverer with all other satellites can be assessed. When the plan is executed, the individual satellite can provide direct observation if the maneuverer provided was effective and provided enough distance. This is a direct and delay reduced confirmation towards the satellite operator.

5.5 Combination of Applications and SSA-Sensor Performance for Concept of Operations

The previous SSA application for star trackers are combined in this concluding section. The ACL is applied here for an ATV-like rendezvous and docking approach to the International Space Station (ISS) (Fig.5-2, green cone). The ATV (Automated Transfer Vehicle) is not in operation anymore and serves here for the Concept of Operations (ConOps)[50-54]. The ConOps is similarly valid and applied to the Cygnus Vehicle [56], the H-II transfer vehicle (HTV) [57] and other crewed and unscrewed vehicles (docking ports are below ISS instead of at the aft side). The Star Tracker in SSA operation mode is enabling a direct, in-orbit monitoring of the perimeter for any object with diameters bigger than 10cm, supporting the controlled approach via the flight path, and predicting the future path of the objects on their orbits and preventing potential hazardous collisions within the ISS Keep-out Zones (KoZ).

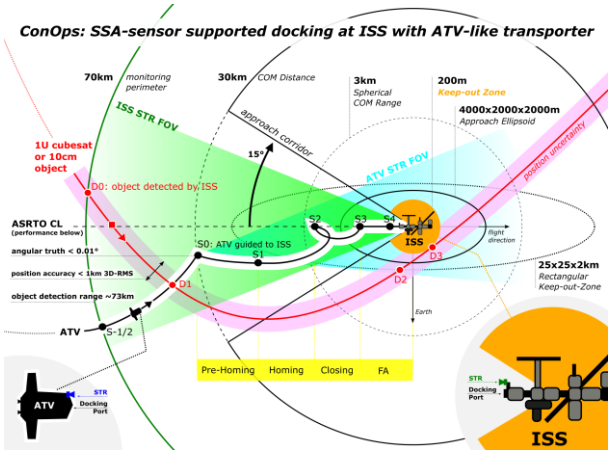

Fig. 5-5: Concept of Operations: SSA-sensor supported docking at ISS with ATV-like transporter.

(zoom image in Appendix A-3) The approach concept is based on that by the ATV and the ISS safety [51] requirements. [50-54] (see Table 5-2 for zone description and requirements)

The presented ConOps is compared to the requirements of the ISS Program safety requirements, which were derived from the existing Shuttle safety policy and requirements [55] and also applied for the Commercial Orbital Transportation Services (COTS) & Commercial Resupply Services (CRS) programs [55] that includes the ATV, Cygnus and H-II vehicles. Figure 5-5 gives a graphical overview and Table 5-2 provides the comparison between the requirements and the ACL star tracker as SSA-sensor performance.

Table 5-2: ACL performance as an SSA sensor comparison to ISS safety requirements and ATV approach.

ISS Safety Requirement[51] and ATV Approach[50-54]	**ISS** requirement	**ACL** performance	Com-pliance
	value (remark)	*value (remark)*	*c/nc*
Trackability			
- *Smallest trackable object (min diameter)*	10cm	10cm (reference)	C*1
- *Data is acquired using […] and space-based telescopes*	yes (via SSN)	yes (ACL on ISS)	C
Safety			
- *Keep-out Zone*	200m (radius)	<1km (as 3D-RMS accuracy)	(C)*2
- *Rectang. Keep-out Zone*	±2x25x25km (Rd., Dwn-T,Cr.-T)	<1km (as 3D-RMS accuracy)	C
Deploy Verification			
- Non-ISS/VV at lower orbit *apogee of deployed object*	15km below ISS	73km (as range)	C*3
- Non-ISS/VV at higher orbit			C
coelliptic & SMA at	45km above ISS	73km (as range)	C
apogee of deployed object	15km below ISS	73km (as range)	C*3
- Robotic *rectang. Keep-out Zone*	±2x25x25km (Rd., Dwn-T,Cr.-T)	73km (as range)	C
- EVA (if used for deploy!) *clearance, unobstr. view*	30° (half cone)	12.5° (as FoV half cone)	(C)*4
ATV Approach			
- *Approach Corridor View*	15° (half cone)	12.5° (as FoV half cone)	(C)
- *COM Distance*	30km	73km (as range)	C
- *Approach Ellipsoid*	4x2x2km	73km (as range)	C
- *Approach Ellipsoid*	4x2x2km	<1km (as 3D-RMS accuracy)	C

*1 trackability for the ACL is meant as detecting the minimum 10cm object at detection distance. All distances and ranges are for this smallest object to be comparable to the ISS safety requirements.
*2 potentially compliance (c), due to one-arc measurements in experiments and expected improvement due to longer and multiple-arc measurement when installed at ISS
*3 ranges are possible without direct Earth-shine on the ACL detector
*4 compliant with either several ACLs are combined to increase the total FoV, or the WFoV ACL with 68° FoV is used.

Within the ConOps, the ACL is mounted on the ISS at the docking port side. From there, the monitoring, tracking and docking support is provided along the "approach corridor". Furthermore, the ATV-like vehicle also has an ACL star tracker for guiding it towards the ISS when the LiDARs are still out of reach.

When the ATV-like vehicle is approaching via the waypoints S-1/2 to S4, the ISS star tracker as an SSA-sensor can fully support the operation. The 25° FoV is almost fully covering the approach corridor and the distances and position offsets are within the ISS STR

FoV (green) from the coasting phase at waypoint S-1/2 to the final docking after S4. If a wider FoV is needed one star tracker with wider FoV is possible or two ISS STR are installed at the ISS. Within the flight path tunnel of the ATV-like (whitened) the position as well as the angular offset towards the ATV are established at the ISS. Likewise, the ATV-like can establish both fundamental parameters. Thus, either both rendezvous via independent open-loops, or when in communication range both can coordinate with closed loop controls of the rendezvous proceeding.

For any 10 cm object (Fig.5-5, red flight path) within the ISS STR FoV, the flightpath can be tracked. Either when an object is initially detected at point D0 at the maximum range of the ACL star tracker for 10cm diameter objects, or when the ATV-like as a "Visiting Vehicle" is deploying (Table 5-2) an object (like a 1U cubesat). Beyond detecting and tracking, the ISS data enables future estimates of the object's flight path. At point D1 the object assessment could reveal a likely collision with the ATV-like. At point D2, the safety requirement of the ISS for deployed objects could be broken. And at point D3, the 3D-position accuracy of the ACL (<1km 3D-RMS) could reveal an imminent collision hazard from the object because it is predicted to be within the KoZ (radius of 200m around the ISS). The ACL as an SSA-sensor is almost fully compliant to the ISS safety requirements (Table 5-2)

Commercial star trackers with ACL like performance, have the performance potential to provide SSA-features for satellite, asset and life protection. They are enabling higher autonomy and safety not just for the ISS or the next-generation space stations, but also for any other satellite and transporter (crewed / unscrewed).

6. Conclusions

We have shown that a commercial the ASTRO CL as a commercial star tracker has demonstrated the capacity and capabilities to detect and track RSO. It is shown that the angular position precision is better than 0.01° considering the reference satellite's TLEs of LEO satellites. As a representative of its class for other commercial star trackers (CST), SSA sensors based on star trackers have the performance needed by missions for space-based sensors as well as for ground based telescope sensor networks. The ASTRO CL is capable of even higher performance by adapting the configuration to the findings of this real-sky measurements by calibration.

Norming the measured data to a 10cm diameter object, two capabilities are revealed. Even fainter objects in GEO are possible to be detected. And satellites in RPO can be counteracted on with a warning time of when it reaches a distance of 73km to the ACL. It is revealed that a common object size for targets is helpful to the community for system trade-offs in the conceptual and design phase of mission and satellite design.

The ASTRO CL demonstrated preliminary orbit determination position accuracy of few km to a few hundred meters in 3D-RMS, with the potential to even better (smaller 3D-RMS) results for positioning and predicting the RSO on its orbit. This is an important performance criteria for SSA applications. All this is possible with the ASTRO CL being able to provide attitude solutions for each frame with 5Hz. The ASTRO CL can serve as a star tracker for the AOCS and in parallel run as a SSA sensor.

The ASTRO CL enables a set of SSA applications, such as Satellite Protection, Sustainable & Clean Space, Navigation, and Space Surveillance Networks & Space Traffic Management. Especially the support of rendezvous and docking of crewed and un-crewed transfer vehicles and in-orbit servicer missions are enabled within the strict safety requirements of the International Space Station standards.

Acknowledgements

Many thanks to the Jena-Optronik team in engineering, production and test who established together the product and a production line throughput capacity of up to 100 units per month.

Related

Further applications and mission concepts for the ASTRO CL as an SSA sensor are presented in a parallel session "B4.3 Small Satellite Operations" during the IAA Small Satellite Symposium during the International Astronautical Congress (IAC2024). There, the PRINCESS team [31] of the TU Berlin present their mission operation concept (Paper Code: IAC-24,B4,3,7,x86584, 2024-10-15 at 15:00 CEST, Space Hall 2)[31].

Acronyms/Abbreviations

3D-RMS	3D Root Mean Square
6-DoF	6 degrees of freedom
AAD	Autonomous Attitude Determination
ACL	ASTRO CL star tracker
Acq.	Acquisition
ACS	average cross section
AOCS	Attitude and Orbital Control System

APS	Active Pixel Sensor
ATV	Automated Transfer Vehicle
C/NC	compliance / non-compliance
CAM	camera
CAD	computer aided design
COM	communication
ConOps	Concept of Operations
COTS	Commercial Orbital Transportation Services
CRS	Commercial Resupply Services
CST	commercial star tracker
CL	ConstelLation
COSPAR	Committee on Space Research
DEB	debris
Ecc	Eccentricity
ESA	European Space Agency
EVA	Extra Vehicular Activity
FA	Final Approach
FoV	field of view
GAO	United States Government Accountability Office
GEO	Geo stationary/synchronous orbit
GMAT	NASA General Mission Analysis Tool
ID	Identification
Inc	Inclination
ISS	International Space Station
JOP	Jena-Optronik GmbH
KoZ	Keep-out Zone
LEO	Low Earth Orbit
LiDAR	Light Detection And Ranging
MEO	Medium Earth Orbit
NAT	Nominal Attitude Tracking
NAV	Navigation
OD	Orbit Determination
RaaN	Right ascension of the ascending node
RA/DEC	Right Ascension / Declination
Rad-hard	radiation hard
RADAR	Radio Detection And Ranging
Rd., Dwn-T,Cr.-T	Radial, Down- & Cross-Track
R/B	rocket body
ROM	rough order of magnitude
RPO	Rendezvous and Proximity Operations
RSO	Resident Space Objects
S/C	spacecraft
SDA	Space Domain Awareness
SNR	Signal-to-Noise ratio
SSA	Space Situational Awareness
SSN	Space Surveillance Network
STM	Space Traffic Management
STR	star tracker
TBA	to be assigned
TDP-6	Technology Demonstrator Payload 6 (JOP ASTRO APS on Alphasat[09])
TLE	Two-Line Element
UTC	Coordinated Universal Time
UTNG	Unit Tester Next Generation PC
vis	visible spectrum or visual
VV	visiting vehicle
XP	eXtreme Precision
X-sect.	cross section, see ACS

References

*Note: All URLs within the references marked with * are accessed on 2024-08-31.*

[01] Jena-Optronik GmbH, *Otto-Eppenstein-Straße 3, 07745 Jena, Germany.* http://www.jena-optronik.de, *

[02] Space-Track.org, data provider is 18th Space Defense Squadron, US-SpaceForce, executes command and control of the U.S. Space Surveillance Network (SSN), https://www.space-track.org, *

[03] "TECHNOLOGY ASSESSMENT - Large Constellations of Satellites - Mitigating Environmental and Other Effects", Sept. 2022, United States Government Accountability Office (GAO), https://www.gao.gov/assets/gao-22-105166.pdf , *

[04] "Performance of Northrop Grumman's Mission Extension Vehicle (MEV) RPO Imagers at GEO", Matt Pyrak, Joseph Anderson, Advanced Maui Optical and Space Surveillance Technologies Conference (AMOS), MAUI, HAWAI'I, USA, September 2021, https://dx.doi.org/10.1117/12.2631524 , *

[05] "AI based location estimation using Digital Twins in rendezvous and docking scenarios", A.Kupetza, L.Scheunemann, J.Rossmann, 73rd International Astronautical Congress (IAC2022), Paris, France, September 2022, https://iafastro.directory/iac/paper/id/73070/ext/summary/ , *

[06] ESA DISCOSweb (Database & Information System Characterising Objects in Space), by ESA's Space Debris Office, https://discosweb.esoc.esa.int/, *

[07] "Global Counterspace Capabilities – An Open Source Assessment", Secure World Foundation, April 2024, https://swfound.org/media/207826/swf_global_counterspace_capabilities_2024.pdf , *

[08] "Chinese Military and Intelligence Rendezvous and Proximity Operations", B.Weeden, Secure World Foundation, July 2023, https://swfound.org/media/207605/fs23-02-chinese-rpo_0723.pdf , *

[09] "Autonomous star sensor ASTRO APS: flight experience on Alphasat", CEAS Space Journal 7(2), U.Schmidt, T.Fiksel, A.Kwiatkowski, I.Steinbach, B.Pradarutti, K.Michel, E.Benzi, June 2015, http://dx.doi.org/10.1007/s12567-014-0071-z , *

[10] "ASTRO CL" product page, https://www.jena-optronik.de/products/star-sensors/astro-cl.html, *

[11] "ASTRO CL Star Tracker Best in class for robustness and performance in the harsh constellation orbits", S.Hahn, S.Colditz, U.Schmidt, S.Schwarz, ESA/CNES 4S Symposium (Small Satellites Systems and Services), Palma de Mallorca, Spain, 2024, https://www.researchgate.net/publication/382732046_ASTRO_CL_Star_Tracker_Best_in_class_for_robustness_and_performance_in_the_harsh_constellation_orbits , *

[12] "High-Accuracy Star Tracker ASTRO XP", ESA 12th International Conference on Guidance Navigation and Control and 9th International Conference on Astrodynamics Tools and Techniques, U.Schmidt, R.Würl, M.Griebel, I.Steinbach, J.Reichardt, D.Adolf, T.Kühn, S.Kirschstein, July 2020, http://dx.doi.org/10.5270/esa-gnc-icatt-2023-056 , *

[13] "Precise In-Orbit Collision Prediction and Space Environment Surveillance System", S.Grau, A.J.Große Siestrup, V.Koßack, J.Plewe, V.Schulz, N.Solak, J.E.C.Teuchert, A.Hornig, E.Stoll, ESA 4S Symposium (Small Satellites Systems and Services), Palma de Mallorca, Spain, 2024, https://www.researchgate.net/publication/381708528_Precise_In-Orbit_Collision_Prediction_and_Space_Environment_Surveillance_System , *

[14] "Precise In-Orbit Collision Prediction and Space Environment Surveillance System" (Poster), S.Grau, A.J.Große Siestrup, V.Koßack, J.Plewe, V.Schulz, N.Solak, J.E.C.Teuchert, A.Hornig, E.Stoll, ESA 4S Symposium (Small Satellites Systems and Services), Palma de Mallorca, Spain, 2024, https://www.researchgate.net/publication/381860253_PRecise_IN-orbit_Collision_prediction_and_space_Environment_Surveillance_System , *

[15] "Enabling general orbital transparency by open-source orbit-determination of CubeSats and other sources", A.Hornig, D.Fritsch, T.Roth, A.Pak, International Astronautical Congress, IAC Cyber Space Edition (IAC2020), October 2020, https://www.researchgate.net/publication/365451516_Enabling_general_orbital_transparency_by_open-source_orbit-determination_of_CubeSats_and_other_sources, *

[16] "Starlink Generation 2 Mini Satellites: Photometric Characterization", A.Mallama, R.Cole, S.Harrington, A.Hornig, J.Respler, A.Worley, R.Lee, June 2023, http://dx.doi.org/10.48550/arXiv.2306.06657 , *

[17] "Spaced based sensor suite for Space Situational and Space Domain Awareness applications", T.Haarlammert, A.Hornig, S.Chelkowski, F.Bouillon, T.Hennig, DLRK2023 (Deutscher Luft- und Raumfahrt Kongress @ DLRG), Stuttgart, Germany, 2023, https://www.researchgate.net/publication/374847987_Spaced_based_sensor_suite_for_Space_Situational_and_Space_Domain_Awareness_applications , *

[18] „Tracking all satellites: adding time-synchronization to each groundstation in a network during post-processing by applying data fusion of signals and time-sources", A.Hornig, D.Fritsch, V.Chandrasekhar, F.L.Gomez-Cortes, 70th International Astronautical Congress (IAC2019), Washington D.C., USA, October 2019, https://www.researchgate.net/publication/365318548_Tracking_all_satellites_adding_time-synchronization_to_each_groundstation_in_a_network_during_post-processing_by_applying_data_fusion_of_signals_and_time-sources , *

[19] "Using satellites' communication preambles as natural fingerprints for satellite identification and positioning (SIDPOS) for orbit tracking and space traffic management", A.Hornig, D.Fritsch, 73rd International Astronautical Congress (IAC2022), Paris, France, September 2022, https://www.researchgate.net/publication/366192145_Using_satellites'_communication_preambles_as_natural_fingerprints_for_satellite_identification_and_positioning_SIDPOS_for_orbit_tracking_and_space_traffic_management , *

[20] B. Rhodes, in SkyField, Elegant Astronomy for Python, https://rhodesmill.org/skyfield/,*

[21] "AUTO-TDS: Enabling laser communication networks to auto detect incoming links, securing connection and auto-routing the data", A.Hornig, K.Treichel, F.Kröber, L.Bohne, F.Bouillon, R.Berger, S.Chelkowski, 73rd International Astronautical Congress (IAC2022), Paris, France, September 2022, https://www.researchgate.net/publication/364459515_AUTO-TDS_ENABLING_LASER_COMMUNICATION_NETWORKS_TO_AUTO_DETECT_INCOMING_LINKS_SECURING_CONNECTION_AND_AUTO-ROUTING_THE_DATA , *

[22] "GeoTracker - a worldwide optical network for Space Situational Awareness", M.Pyanet, L.Hennegrave, S.Vourc, et al., 2017, https://www.semanticscholar.org/paper/GeoTracker-a-worldwide-optical-network-for-Space-Pyanet-Hennegrave/16bfd70fe7b63e16e937955a58a12bc701c08b61 , *

[23] "Analysis of the angle-only orbit determination for optical tracking strategy of Korea GEO satellite, COMS", J.Choi, J.h.Jo, K-M.Roh, et al., Advances in Space Research, June, 2015, https://www.researchgate.net/publication/282619859_Analysis_of_the_angle-

only_orbit_determination_for_optical_tracking_strategy_of_Korea_GEO_satellite_COMS , *

[24] "Non-Traditional Data Collection and Exploitation for Improved GEO SSA via a Global Network of Heterogeneous Sensors", J.Aristoff, N.Dhingra, A.Ferris, A.Hariri, et al., Advanced Maui Optical and Space Surveillance Technologies Conference (AMOS), MAUI, HAWAI'I, USA, 2018, https://amostech.com/TechnicalPapers/2018/Optical-Systems_Instrumentation/Aristoff.pdf , *

[25] "A New Approach to Space Situational Awareness using Small Ground-Based Telescopes – Final Report", NC.Anheier, C.Chen, December 2014, https://www.pnnl.gov/main/publications/external/technical_reports/PNNL-23994.pdf , *

[26] "Tracking Merged Objects within Non-Resolved Imagery", C.Meredith, P.Chote, R.Airey, Advanced Maui Optical and Space Surveillance Technologies Conference (AMOS), MAUI, HAWAI'I, USA, 2023 https://amostech.com/TechnicalPapers/2023/Satellite-Characterization/Meredith.pdf , *

[27] "Canadian Photometric Measurements During the Multinational Phantom Echoes Space Situational Awareness Experiment", L.Scott, S.Thorsteinson, 2020, https://casi.ca/resources/Documents/ASTRO/2020/Canadian%20Space%20Based%20Observations%20FIndings%20during%20the%20Phantom%20Echoes%20Experiment%20R3.pdf , *

[28] "PHANTOM ECHOES 2: A Five-Eyes SDA Experiment on GEO Proximity Operations", P.Chote, L.Scott, J.Skuljan, J.Alvino, J.Firth, Advanced Maui Optical and Space Surveillance Technologies Conference (AMOS), MAUI, HAWAI'I, USA, 2021, https://amostech.com/TechnicalPapers/2021/Conjunction-RPO/George.pdf , *

[29] "Large phase angle observations of GEO satellites", R.L.Cognion, SPIE Defense, Security and Sensing, May 2013, http://dx.doi.org/10.1117/12.2014623 , *

[30] "Stability Analysis of LEO Rocket Bodies", T.W.Stromberg, K.A.Wilson, T.bate, F.K.Chun, D.M.Strong, D.McKnight, dvanced Maui Optical and Space Surveillance Technologies Conference (AMOS), MAUI, HAWAI'I, USA, 2023, https://amostech.com/TechnicalPapers/2023/Poster/Stromberg.pdf , *

[31] "Mission Operations for Precise In-Orbit Collision Prediction and Space Environment Surveillance", S.Grau, D.Roychowdhury, S.Kapitloa, E.Stoll, 75th International Astronautical Congress (IAC2024), Milan, Itally, October 2024, https://www.researchgate.net/publication/385242740_Mission_Operations_for_Precise_In-Orbit_Collision_Prediction_and_Space_Environment_Surveillance_System , *

[32] OrbitDeterminator, from the Distributed Ground Station Network (DGSN) project, MIT license, Github.com, https://github.com/aerospaceresearch/orbitdeterminator , *

[33] "Distributed Ground Station Network - a global system for tracking and communication with small satellites as an open service", A.Hornig, T.Eversmeyer, U.Beyermann, International Astronautical Congress (IAC2023), Beijing, China, 2013, https://www.researchgate.net/publication/258207922_DISTRIBUTED_GROUND_STATION_NETWORK_-_A_GLOBAL_SYSTEM_FOR_TRACKING_AND_COMMUNICATION_WITH_SMALL_SATELLITES_AS_AN_OPEN_SERVICE , *

[34] "An Overview of the ARTEMIS I Navigation Performance", G.Holt, C.D'Souza, M.Wasinger, 45th Annual AAS Guidance, Navigation and Control (GN&C) Conference, Breckenridge, CO, USA, 2023, https://ntrs.nasa.gov/citations/20230000714 , *

[35] "ASTRO APS3" product page, https://www.jena-optronik.de/products/star-sensors/astro-aps.html; *

[36] "ASTRO XP" product page, https://www.jena-optronik.de/products/star-sensors/astro-xp.html , *

[37] "SSA Sensor Suite" product page, https://www.jena-optronik.de/products/cameras-and-camera-systems/ssa-sensor-suite.html, *

[38] "LIDAR" product page, https://www.jena-optronik.de/products/rendezvous-sensors/applications.html , *

[39] "Understanding the Impact of Satellite Constellations on Astronomy", IAU2001, Press Release, 12th February 2020 , https://www.iau.org/news/pressreleases/detail/iau2001/ , *

[40] "Multicolor and multi-spot observations of Starlink's Visorsat", Takashi Horiuchi, Hidekazu Hanayama, Masatoshi Ohishi, et al., Publ. Astron. Soc. Japan (2023) 00 (0), 1–23 , in 2023, http://dx.doi.org/10.1093/pasj/psad021 , *

[41] Interactive Presentation of this paper, https://iac2024-iaf.ipostersessions.com/default.aspx?s=52-A5-8C-C6-71-F0-C6-99-10-0A-B9-76-93-20-69-E0 , *

[42] "Technical challenges of the Debris Deorbit Demonstrator and Envisat Observation Satellite (D3EOS) mission", A.Fecht, S.Latzko, T.Mayer, M.Mundiger, M.Schwinning, 66th International Astronautical Congress (IAC2015), Jerusalem, Israel, Oct 2015, https://www.researchgate.net/publication/283343583_Technical_challenges_of_the_Debris_Deorbit_Demonstrator_and_Envisat_Observation_Satellite_D3EOS_mission , *

[43] "The QUEEN Mission to Demonstrate an Optical Rb Frequency Reference Payload and Advanced Small Satellite Platform Technology", M.Barschke, A.N.Dinkelaker, A.Bawamia, et al., 70th International Astronautical Congress (IAC2019), Washington D.C., USA, October 2019, https://www.researchgate.net/publication/358495401_The_QUEEN_Mission_to_Demonstrate_an_Optical_Rb_Frequency_Reference_Payload_and_Advanced_Small_Satellite_Platform_Technology , *

[44] "Status on laser communication activities at Tesat-Spacecom", M.Gregory, F.Heine, A.Brzoska, K.Oestrich, P.Martin-Pimentel, H.Zech, R.Mahn, SPIE LASE, 2024, San Francisco, California, USA, 12th March 2024, http://dx.doi.org/10.1117/12.3001511 , *

[45] "Final Series of Northrop Grumman-Built C-Band Satellites Successfully Launch", Laura Keefe, news-release, 17th March 2023, https://news.northropgrumman.com/news/releases/final-series-of-northrop-grumman-built-c-band-satellites-successfully-launch , *

[46] "Mitigation of LEO Satellite Brightness and Trail Effects on the Rubin Observatory LSST", J.A.Tyson, Z.Ivezic, A.Bradshaw, et. al., The Astronomical Journal, Volume 160, Number 5, 27th. October 2020, http://dx.doi.org/10.3847/1538-3881/abba3e , *

[47] "Satellite Optical Brightness", F.Frankhauser, J.A.Tyson, J.Askari, The Astronomical Journal, Volume 166, Number 2, 13th July 2023, http://dx.doi.org/10.3847/1538-3881/ace047 , *

[48] "Brightness Mitigation Best Practices for Satellite Operators", SpaceX 2022, https://api.starlink.com/public-files/BrightnessMitigationBestPracticesSatelliteOperators.pdf , *

[49] "Impact of Satellite Constellations on Optical Astronomy and Recommendations Toward Mitigations", NOIRLab, AURA, American Astronomical Society, 25th August 2020, https://noirlab.edu/public/products/techdocs/techdoc003/ , *

[50] "ATV: Rendezvous with ISS", H.Wartenberg, P.Amodieu, ESA "on station no. 11", p.17-19, December 2002, https://www.esa.int/esapub/onstation/os11.pdf , *

[51] "ISS Safety Requirement Document, International Space Station Program, SSP 51721 Baseline", NASA, September 2019, https://ntrs.nasa.gov/api/citations/20210009936/downloads/SSP%2051721-Baseline.pdf , *

[52]"Communication/Exploration/Navigation Technologies – Applications, Trade-Offs and possible Transfers between Space and Ground at the Example of MOA², a novel pulsed Plasma Accelerator", Norbert Frischauf, Technical University Graz, July 2014, https://www.researchgate.net/publication/304579802_CommunicationExplorationNavigation_Technologies_-_Applications_Trade-Offs_and_possible_Transfers_between_Space_and_Ground_at_the_Example_of_MOA_a_novel_pulsed_Plasma_Accelerator , *

[53]"Rendezvous Lidar Sensor System for Terminal Rendezvous, Capture, and Berthing to the International Space Station", A.C.M. Allen, C.Langleya, R.Mukher, Proc. of SPIE Vol. 6958 69580S-12008 SPIE Digital Library, April 2008, http://dx.doi.org/10.1117/12.777208 , *

[54] "ATV Johannes Kepler: Rendezvous & docking – step by step", D.Scuka, ESA Blog, 23rd February 2011, https://blogs.esa.int/orion/2011/02/23/atv-johannes-kepler-rendezvous-docking-step-by-step/ , *

[55] "RISK MITIGATION APPROACH TO COMMERCIAL RESUPPLY TO THE INTERNATIONAL SPACE STATION", D.S.Koons, C.Schreiber, F.Acevedo, M.Sechrist, International Association for the Advancement of Space Safety: "Making Safety Matter", May 2010, https://ntrs.nasa.gov/api/citations/20100014822/downloads/20100014822.pdf , *

[56] "Designing and Validating Proximity Operations Rendezvous and Approach Trajectories for the Cygnus Mission", P.Miotto, L.Breger, I.Mitchel, B.Keller, B.Rishikof, AIAA Guidance, Navigation, and Control Conference, August 2010, http://dx.doi.org/10.2514/6.2010-8446 , *

[57] "Automatic Rendezvous to the International Space Station", Jun Tsukui, Shigeki Hotta, Takane Imada, Koji Yamanaka, Toru Kasai, 7th International Symposium on Artificial Intelligence, Robotics and Automation in Space: i-SAIRAS 2003, NARA, Japan, May 19-23, 2003, https://robotics.estec.esa.int/i-SAIRAS/isairas2003/data/pdf/AS15paper.pdf , *

[58] "Cubesat positioning performance comparison between on-board GNSS, active 1-way ranging and TDOA methods by the Distributed Ground Station Network, and the resulting time from rideshare launch to identification - An operator's selection help", A.Hornig et al., 75th International Astronautical Congress (IAC2024), Milan, Italy, 16th of October 2024, https://iafastro.directory/iac/paper/id/90993/summary/ , *

[59] "Assessment of Brightness Mitigation Practices for Starlink Satellites", A.Mallama, R.Cole, S.Harrington, A.Hornig, J.Respler, A.Worley, R.Lee, Oct 2023, https://arxiv.org/abs/2309.14152 , *

[60] "Satellites to be Built & Launched by 2030 – an extract - A complete analysis & forecast of the

satellite manufacturing & launch service markets", 24th edition, Novaspace (former Euroconsult), December 2021, https://digital-platform.euroconsult-ec.com/wp-content/uploads/2022/01/Extract_Sat_Built_2021.pdf , *

[61] "Satellite manufacturing and launch services: trends and forecasts 2023–2033", analysis mason, 12th July 2024, https://www.analysysmason.com/what-we-do/capabilities/space/ , *

[62] "Aerospace & Defense Practice - Large LEO satellite constellations: Will it be different this time?", McKinsey & Company, May 2020, https://www.mckinsey.de/~/media/McKinsey/Industries/Aerospace%20and%20Defense/Our%20Insights/Large%20LEO%20satellite%20constellations%20Will%20it%20be%20different%20this%20time/Large-LEO-satellite-constellations-Will-it-be-different-this-time-VF.pdf , *

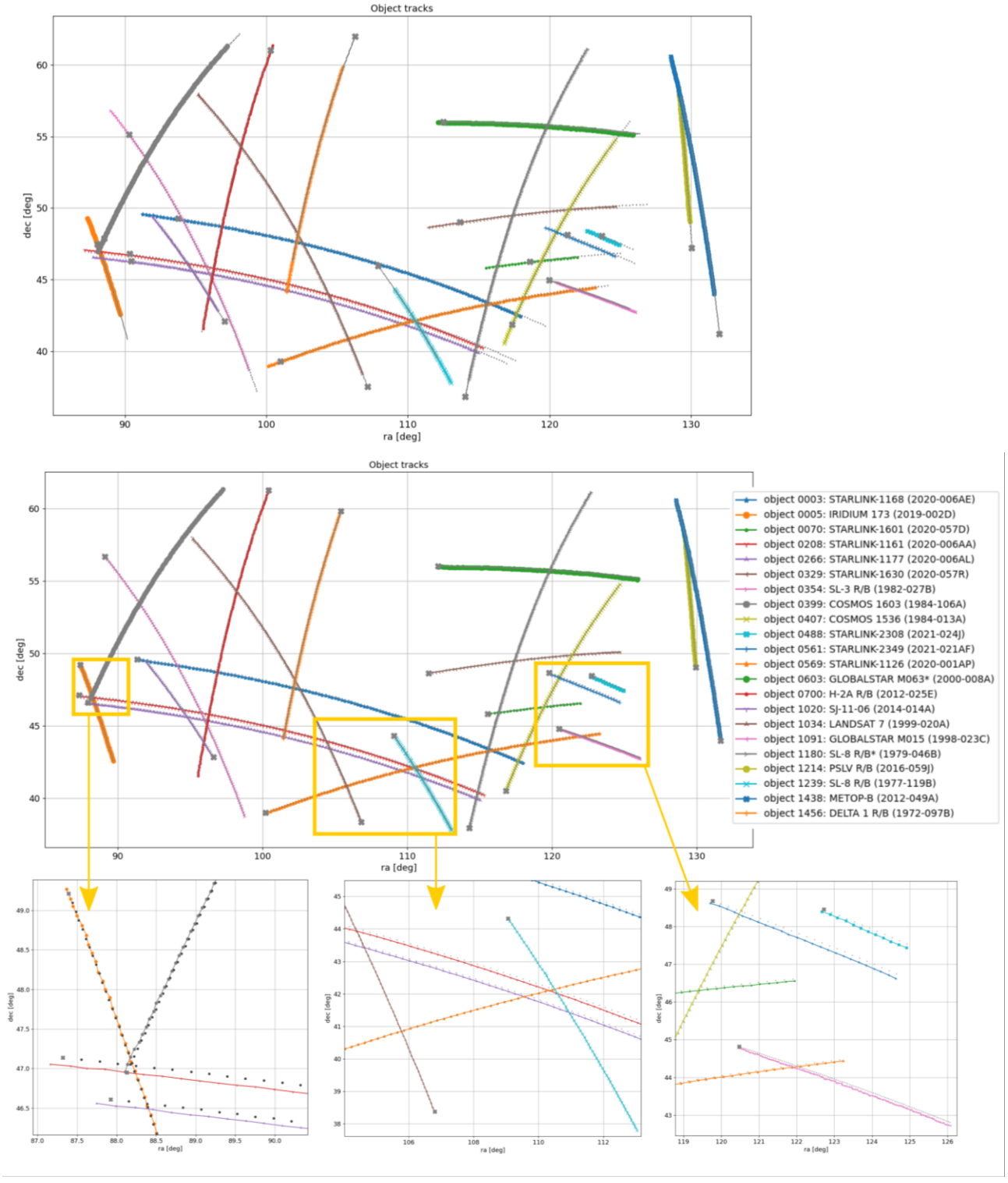

Fig. A-1: Tracks in RA/DEC. Satellite tracks by TLE (dots) closely matching the measured tracks. The X marks the first RA/DEC position of the satellite track (zoomed view for Figure 4-6)

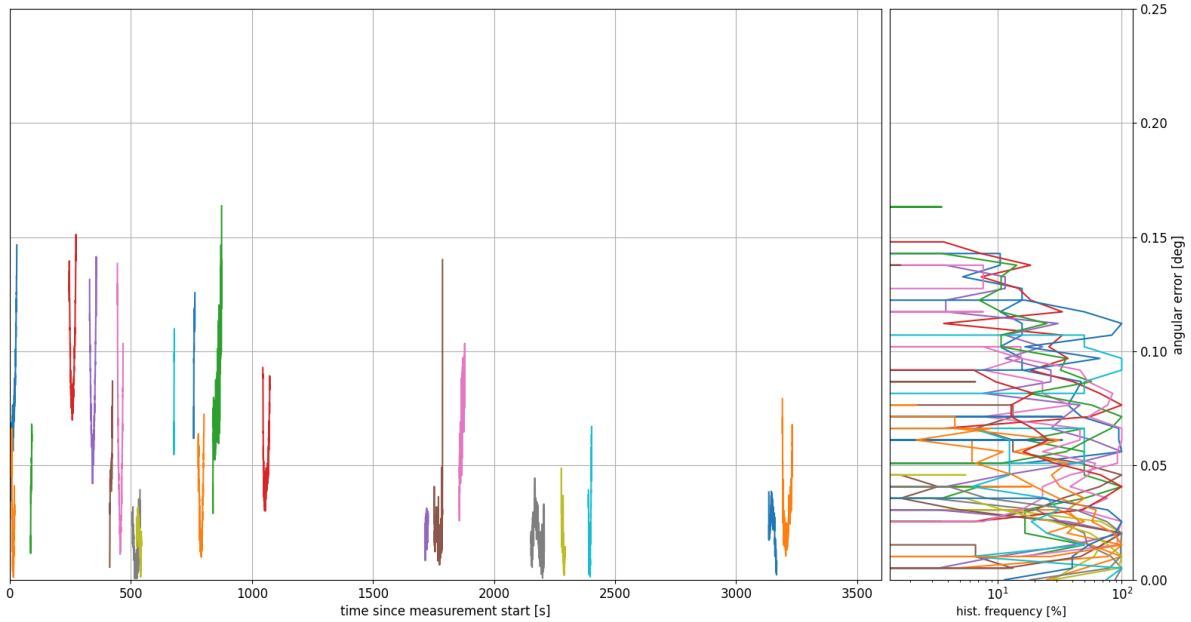

Fig. A-2: Angular distance error (angular truth) over time (left) and their histograms (right). The error reaches 0.01° precision (zoomed view for Figure 4-7)

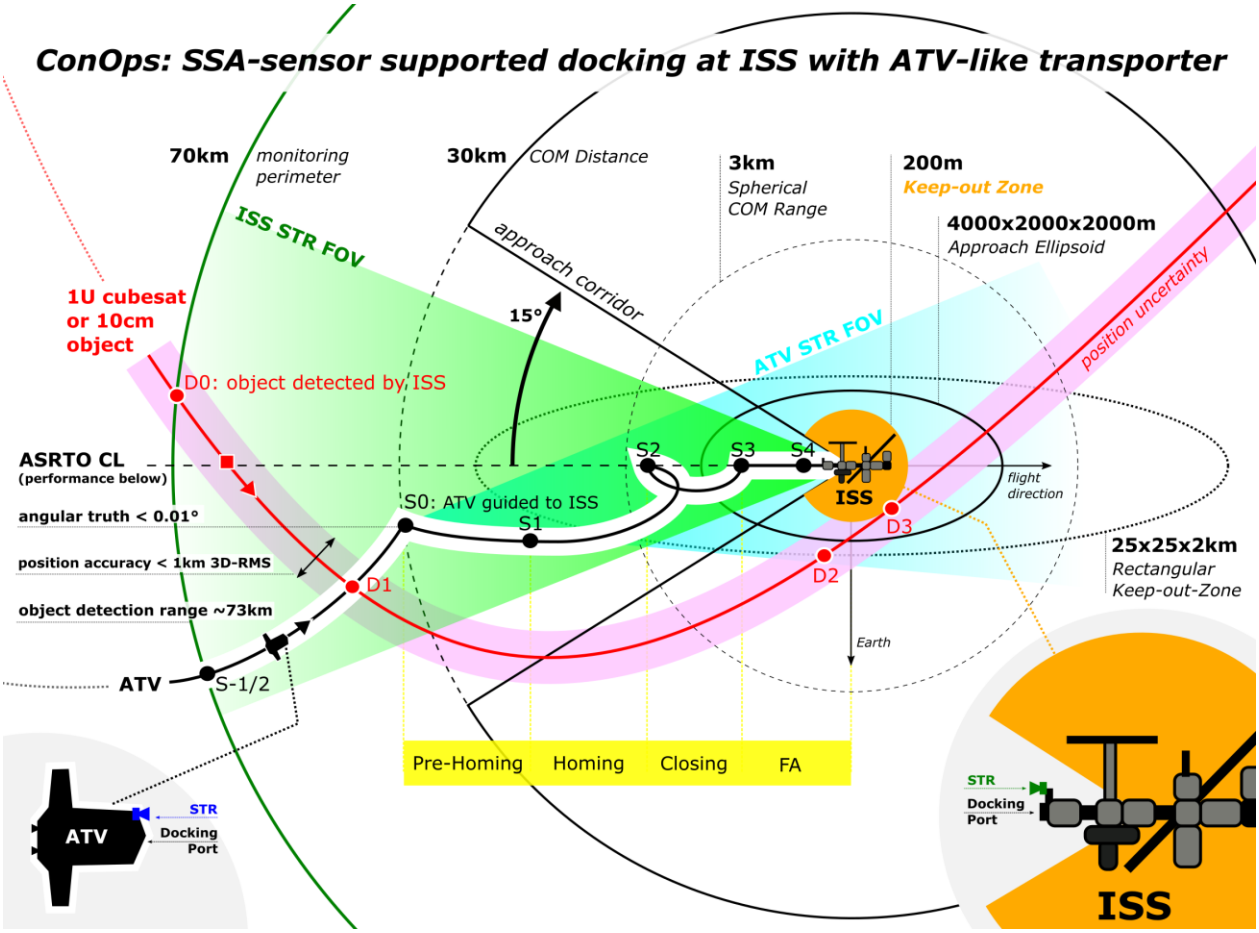

Fig. A-3: Concept of Operations: SSA-sensor supported docking at ISS with ATV-like transporter. (zoomed view for Fig. 5-5)